U.S. DEPARTMENT OF ENERGY | Office of Science

DOE/SC-CM-24-003

FY 2024 Third Quarter Performance Metric: Demonstrating and Evaluating Sub-Kilometer Regional-to-Urban Integrated Pluvial and Fluvial Flooding Simulations Driven by Kilometer-Scale Extreme Event Precipitation

Ning Sun
Lead Author

Preston Spicer
Mithun Deb
Zhaoqing Yang
Cade Reesman
Youngjun Son
David Judi
Contributing Authors

July 2024

DISCLAIMER

Contents

Figures

1.0 Product Definition

Flooding is one of the costliest natural hazards, inflicting billions of dollars in annual damages.[1–3] Low-lying coastal areas are particularly prone to a range of flood hazards, including direct runoff from heavy rainfall (pluvial flood), river flooding (fluvial flood), and coastal storm surges and high tides (coastal flood). When these flood drivers overlap spatially or temporally, they can lead to "compound flooding", which often results in more severe damage,[4–6] as exemplified by Hurricane Irene (2011) – a storm that caused unprecedented compound flooding in many Mid-Atlantic areas.[7,8] With projected increases in extreme precipitation, intensified hydrological cycle, sea level rise, and continued coastal development, urban coastal populations and infrastructures face escalating risks.[9–13] Accurate flood predictions are crucial for effective flood risk management and resilience strategies in these areas.

Sponsored by the U.S. Department of Energy (DOE), a coastal flood modeling framework (DHSVM-FVCOM-RIFT) has been developed for regional-to-urban integrated modeling of fluvial, pluvial, and coastal flood processes at sub-kilometer spatial resolution. This framework couples regional hydrology (DHSVM[14] – Distributed Hydrology Soil Vegetation Model), coastal hydrodynamics (FVCOM[15] – Finite-Volume Community Ocean Model), and urban hydrodynamics (RIFT[16] – Rapid Infrastructure Flood Tool) models. The term 'sub-kilometer regional-to-urban' refers to simulations that span extensive regional landscapes to detailed urban environments at spatial resolutions from 150 meters to 10 meters. ***In this report, we demonstrate that driven by kilometer- or near-kilometer-scale atmospheric forcing, the DHSVM-FVCOM-RIFT framework skillfully predicts sub-kilometer-scale flooding across river, coastal, and urban systems, even during complex compound flooding events.*** The modeling capability and accuracy are demonstrated in two distinct U.S. coastal areas through: (1) an event-scale modeling of the 2022 compound flooding event in the Puget Sound region and (2) long-term modeling (1985-2019) of integrated fluvial, coastal, and pluvial flooding across the Delaware River, Bay, and Philadelphia. The sub-kilometer modeling capabilities were evaluated for each regional demonstration using available observational data. For example, DHSVM was evaluated using observational streamflow data, FVCOM was evaluated using observational tide gage data, and RIFT was evaluated using observational instream water surface elevation data. For the Puget Sound region in the Pacific Northwest, the modeling focused on a single compound flooding event in 2022. This event, characterized by concurrent king tides, rain-on-snow river flooding, and storm surges, caused extensive flooding across the Puget Sound region, especially in Seattle's Duwamish District. The modeling of this event was conducted using DHSVM-FVCOM-RIFT, driven by 3-km atmospheric forcing from the Simple Cloud-Resolving Energy Exascale Earth System (E3SM) Atmosphere Model (SCREAM) with regional refinement. The modeling framework accurately captured the tidal ranges and timing, as well as influence from storm surges and river discharge. Analysis of tide, river, and surge effects on coastal flooding indicates the importance of modeling the strong nonlinear interactions between the forcing mechanisms.

In the Delaware coastal region, we used the DHSVM-FVCOM-RIFT framework to conduct 35-year continuous simulations of watershed-coastal processes, aiming to provide a more comprehensive evaluation of flood modeling accuracy over extended time scales. Due to the computational demands of generating kilometer-scale atmospheric forcing, we used near-kilometer-scale atmospheric forcing from the WRF-TGW[17] dataset. This dataset offers 12-km, 40-year historical climate simulations that are dynamically downscaled from climate reanalysis data using the Weather Research and Forecasting

(WRF) model. Through extensive evaluations against available observational data, including river discharge, coastal water level, and urban flooding, this modeling framework consistently demonstrates skillful flood prediction across both coastal regions. Notably, we also demonstrate the capability of this framework for property-level assessments of probabilistic flood hazards, flood drivers, and infrastructure flood exposure in Philadelphia. Overall, we found that river flooding plays a significant role in Philadelphia flooding, contributing to 73% of events, either as a single driver or as a component in compound driver cases. We also identified three compound flood events involving concurrent surge, pluvial flooding, and river flooding, highlighting the complexity of flood drivers in Philadelphia and emphasizing the need for models that accurately represent the interactions between multiple flood drivers.

2.0 Product Documentation

This report documents DOE's advanced capability in simulating regional-to-urban flooding from integrated pluvial, fluvial, and coastal impacts, using the DHSVM-FVCOM-RIFT modeling framework. The modeling capability and accuracy are demonstrated in two distinct U.S. coastal areas through: (1) an event-scale modeling of the 2022 compound flooding event in the Puget Sound region, driven by 3-km SCREAM atmospheric forcing; and (2) long-term modeling of integrated fluvial, coastal, and pluvial flooding across the Delaware River, Bay, and Philadelphia, driven by 12-km WRF-TGW climate simulations (1985-2019). More details on the modeling framework, the atmospheric forcing applied, and the coastal regions studied are described below.

2.1 Integrated Flood Modeling Framework

The framework consists of three one-way coupled, process-based models: (1) DHSVM,[14,18] a watershed hydrology model that simulates hydrological processes at a spatial resolution of 90–150 m; (2) FVCOM,[15,19] a 3D coastal hydrodynamic model that simulates coastal storm surges and flooding. Its resolution varies from tens of kilometers along the open ocean boundary to hundreds of meters within river channels; (3) RIFT,[16] a 2D hydrodynamic model that simulates urban flooding at a 10-m resolution. As illustrated in Figure 1, DHSVM generates spatially distributed river discharge, which establishes the river boundary condition for FVCOM at the river-ocean interface. Subsequently, FVCOM generates spatially continuous coastal water levels. Urban flooding is then simulated using RIFT, which uses the outputs from DHSVM and FVCOM as its river and coastal boundary conditions, respectively, at their domain interfaces.

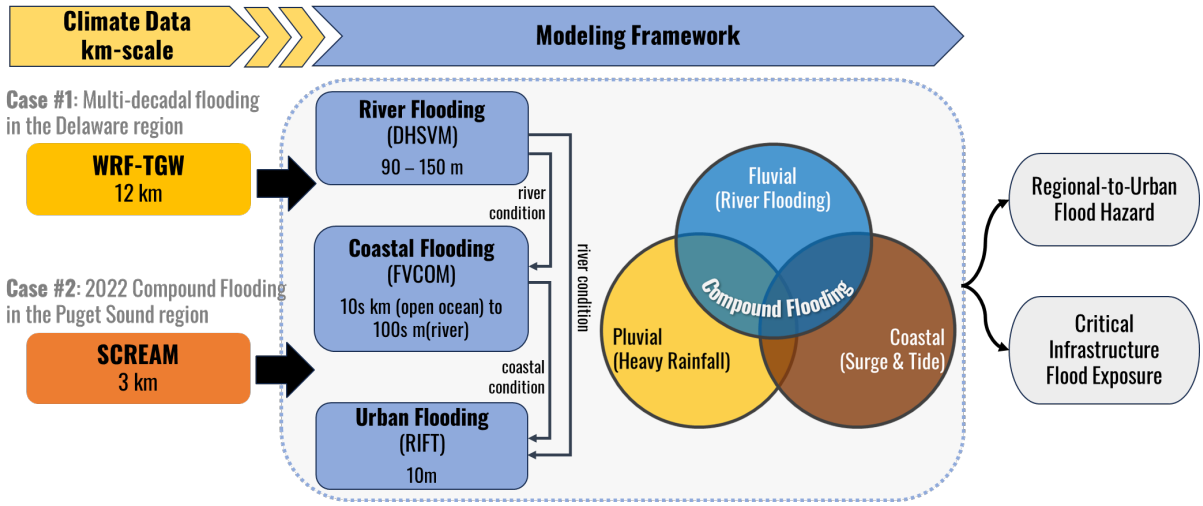

Figure 1. The integrated modeling framework for sub-kilometer regional-to-urban modeling of flood hazards. This modeling capability is demonstrated in two distinct U.S. coastal regions: Puget Sound, driven by 3-km SCREAM atmospheric simulations, and Delaware, driven by 12-km WRF-TGW climate simulations.

2.2 Meteorological Forcing

3-km SCREAM (Puget Sound)

For the 2022 compound flooding events in the Puget Sound, a newer version of SCREAM was used to produce atmospheric forcing for this event, as described in detail in the Q2 metric report. The SCREAM domain features a refined region with 3.25-km grid spacing over the U.S. Pacific Northwest and the northeastern Pacific Ocean within a global domain at 25-km grid spacing. Nudging was applied to grid cells outside the transition zone with grid spacing varying from 3.25 km to 25 km. The updated SCREAM significantly improved the simulation of orographic precipitation in the region. During the 2022 event, SCREAM showed peak precipitation and temperature biases of -10% and 0.16 K, respectively, when compared to observations.

12-km WRF-TGW (Delaware)

The meteorological data for Delaware is sourced from the 1980–2019 historical segment of WRF-TGW climate dataset[17], which is dynamically downscaled from European Centre for Medium-Range Weather Forecasts version 5 re-analysis (ERA5), with a spatial resolution downscaled from ~30 km to 12 km using the WRF model. This dataset provides extensive meteorological variables at hourly and three-hourly resolutions over the contiguous United States. As demonstrated in Jones et al. (2023),[17] WRF-TGW's precipitation patterns align well with the observationally derived Parameter-elevation Regressions on Independent Slopes Model (PRISM)[20]. Notably, it only slightly underestimates the 95th percentile of daily maximum precipitation in the Mid-Atlantic region and generally captures locations of tropical cyclone landfalls, as compared to the International Best Track Archive for Climate Stewardship (IBTrACS)[21] database.

2.3 Distinct Flood Dynamics in Delaware versus Puget Sound

The Delaware and Puget Sound coastal regions are both exposed to flood hazards resulting from a complex interplay of fluvial, pluvial, and coastal processes. However, their distinct geographical and climatic conditions result in unique flood characteristics, making them ideal for evaluating the robustness and transferability of our flood modeling capabilities. The Delaware region (Figure 2a) is characterized by a humid continental climate, where floods are primarily driven by short, intense rainfall events, rain-on-snow, and hurricane landfall typically occurring in late summer and fall.[18,22] When storm surge from hurricanes coincides with heavy rainfall and river flooding, it can lead to severe compound flooding, as exemplified by Hurricane Irene (2011). In contrast, the Puget Sound region with steep mountain terrain (Figure 2b), typically experiences flooding during the winter and spring from heavy precipitation or rain-on-snow events. Extreme flood events are frequently linked to atmospheric rivers (ARs), which produce heavy precipitation and strong winds upon making landfall over mountainous areas such as the U.S. west coast.[23,24] Unlike the Delaware region, king tides are an important driver of coastal inundation in Puget Sound.[19] When king tides coincide with heavy rainfall and river flooding, they create a substantial risk of compound flooding. This was notably the case during the 2022 compound flood event. During this event, the Puget Sound region, particularly the Duwamish area in Seattle, experienced widespread flooding from a combination of king tides, storm surge, and river flooding caused by rain on snow.

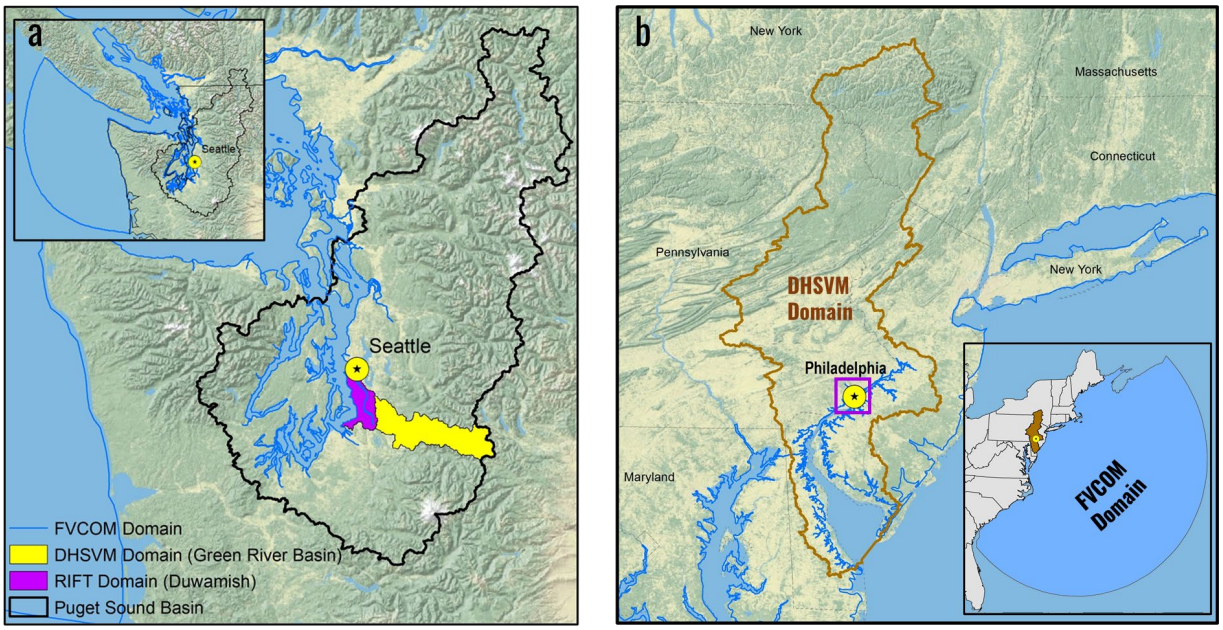

Figure 2. The domains of DHSVM-FVCOM-RIFT for flood modeling in: (a) the Puget Sound region, where DHSVM was configured for the Green River basin, FVCOM domain extends 175 to 250 km offshore of the Olympic Peninsula and a further 300 km inland to South Puget Sound, and the RIFT domain is confined within the HUC12 watershed (ID: 171100130305), which includes the Duwamish area; (b) the Delaware region, where DHSVM was configured for the Delaware River basin, FVCOM domain extends ~700 km offshore from the mid-Atlantic coast and ~215 km upstream from the Delaware Bay mouth, and the RIFT domain covers the City of Philadelphia-Schuylkill River watershed (HUC12: 020402031008).

3.0 Results

3.1 Modeling the 2022 Puget Sound Compound Flood Event

Fluvial and Coastal Flood Modeling Performance

To simulate the compound flood event of December 2022, we used 3-km SCREAM atmospheric simulations as inputs for DHSVM-FVCOM-RIFT. Additionally, we used an ensemble of WRF atmospheric simulations to assess and compare their performance alongside SCREAM in simulating this compound flooding event. For fair comparisons, WRF was configured also at 3-km grid spacing within the regionally refined domain of SCREAM. WRF generated an ensemble of 10 simulations using various combinations of atmospheric physics parameterizations, two land surface models, and two reanalysis boundary conditions (ERA5 and the North American Regional Reanalysis [NARR]).

For river flooding, we evaluated sub-kilometer DHSVM streamflow simulations using gauge observations at the outlet of the Green River Basin (Figure 3). Sub-kilometer simulations driven by SCREAM proved most accurate, achieving a Kling-Gupta Efficiency (KGE) for daily streamflow of 0.77, where a KGE score of 1 indicates perfect agreement. In contrast, the daily KGE for the WRF ensemble varied significantly, ranging from -0.17 to 0.58. Similarly, the mean percent bias for SCREAM-driven simulations was 6.1%, while the WRF ensemble exhibited a broader bias range from -52.1% to 58.6%.

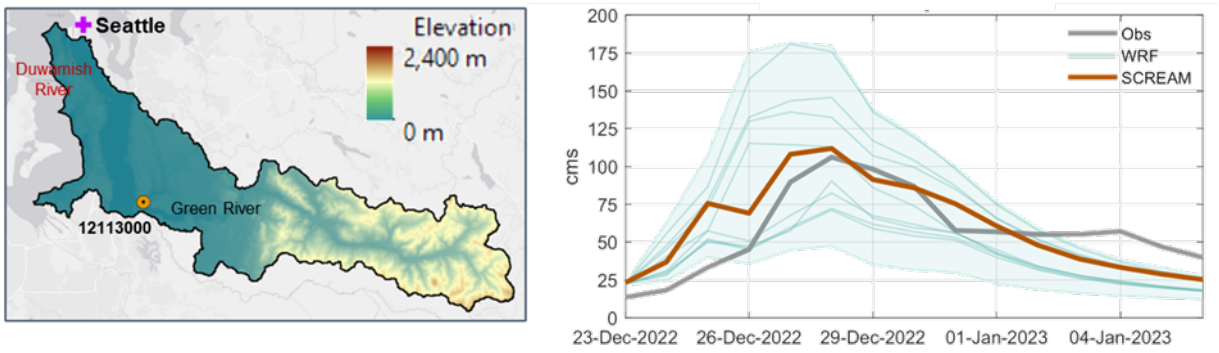

Figure 3. Comparisons of observed streamflow (thick grey line) and DHSVM-simulated streamflow for the December 2022 compound flood event. Observations were taken from a USGS gauge at the outlet of the Green River Basin, the most downstream gauge not influenced by tides, as shown on the left panel where the color shading corresponds to the surface elevation indicated by the color bar. The DHSVM simulations include those driven by the SCREAM simulation (orange line) and an ensemble of WRF simulations (light blue shaded area). The SCREAM-driven streamflow simulations provide the best match to observed streamflows during the event.

For coastal flooding, sub-kilometer Water Surface Elevation (WSE) simulations from FVCOM were evaluated using hourly observations from seven NOAA tide gauges and one USGS tidal river gauge in Duwamish during the event (Figure 4). The results demonstrate strong agreement, with correlation coefficients ranging from 0.93 (Duwamish) to 0.99 (Neah Bay), and the mean bias ranging from -0.4 m (Tacoma) to -0.05 m (Neah Bay). Tidal ranges and timing are accurately captured, as well as influence from storm surges and river discharge.

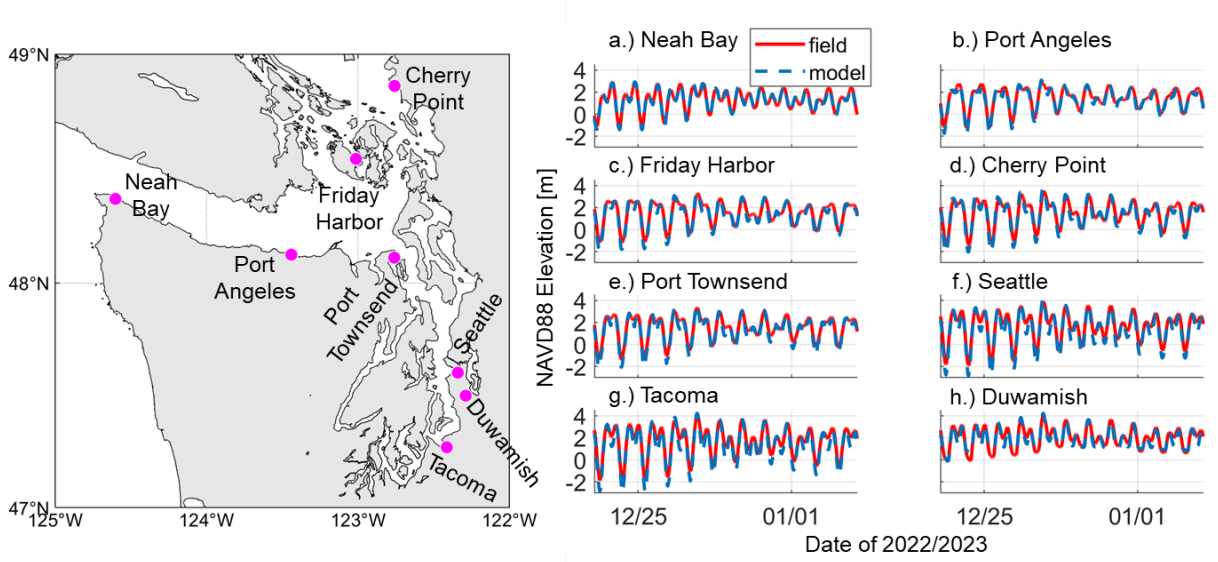

Figure 4. Comparison of FVCOM-simulated water surface elevations with eight NOAA tide gauge observations for the December 2022 compound flood event, as shown on the left map.

Analysis of Tide, River, and Surge Effects on Coastal Flooding

The relative contributions of tides, surge, and river flow to total water levels (TWL) are analyzed between Duwamish and Seattle locations (Figure 5). The Duwamish location is 12 km upstream of Seattle, near the mouth of the estuary. We compared simulated water level from isolated effects of tide, surge, and river forcings, each simulated independently in models with all other forcings turned off. The simulation combining all forcings provided comprehensive TWL simulations, which show significant differences between Seattle and Duwamish, primarily manifested in higher low waters at Duwamish (Figure 5a). This variation is partly due to tidal effects, which display similar high waters but distinct low waters at each location (Figure 5b). More importantly, river contributions to Duwamish range from 1.6–2.5 m, yet are minimal at Seattle (Figure 5d), illustrating significant spatial variability in river-driven water levels. Storm surge, generated both remotely and locally in Puget Sound, peaks near 1.8 m. However, it affects both locations nearly equally, suggesting that surge impacts are rather spatially consistent across the region (Figure 5c). Further, the summed maximum water levels from tide-only, surge-only, and river-only simulations at Duwamish do not match the maximum TWL, suggesting strong nonlinear interactions between the forcing mechanisms that are important to model.

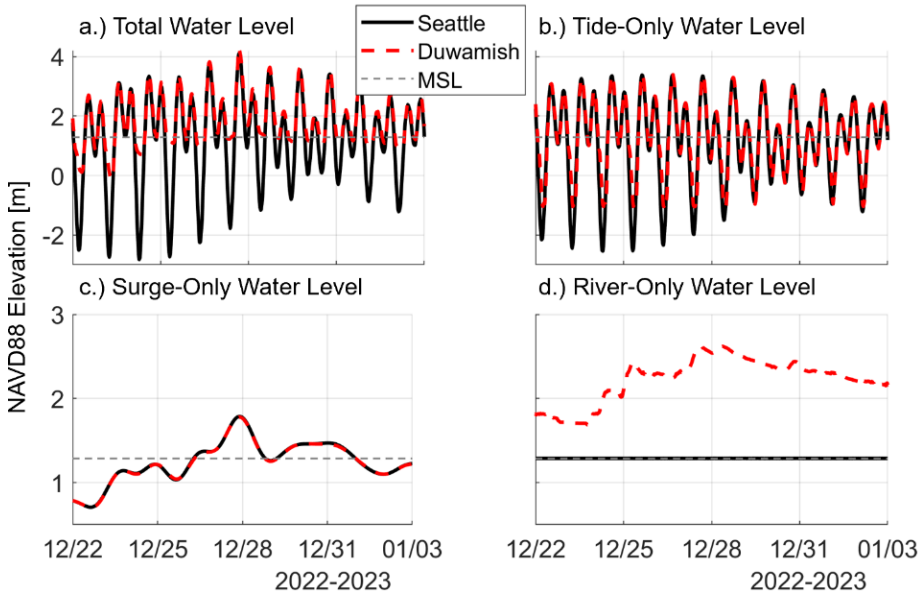

Figure 5. Comparison of FVCOM-simulated water surface elevations for the December 2022 compound flood event at the Seattle (black) and Duwamish (dashed red) gauge locations for four forcing sensitivity runs: (a) total water levels from combined tide, surge, and river forcings, (b) water level from tide-only simulation, (c) water level from surge-only simulation, and (d) water level from river-only simulation, indicating significant spatial variability in river-driven water levels. Mean sea level (MSL) is indicated in each panel (dashed gray).

Modeling Urban Flooding

We ran the RIFT model at a 10-meter resolution to simulate urban flooding during the compound event for the HUC12 watershed (ID: 171100130305), which includes areas of Duwamish near Seattle that experienced significant flooding. The river/coastal boundary forcing for RIFT were provided by DHSVM/FVCOM. Although the absence of high-water mark measurements and in-channel water depth data within the domain precluded a detailed evaluation of RIFT, the model's simulations (Figure 6) align broadly with publicly available reports that indicate approximately two feet of flooding in some Duwamish neighborhoods (e.g., near the west bank of the lower Duwamish waterways).

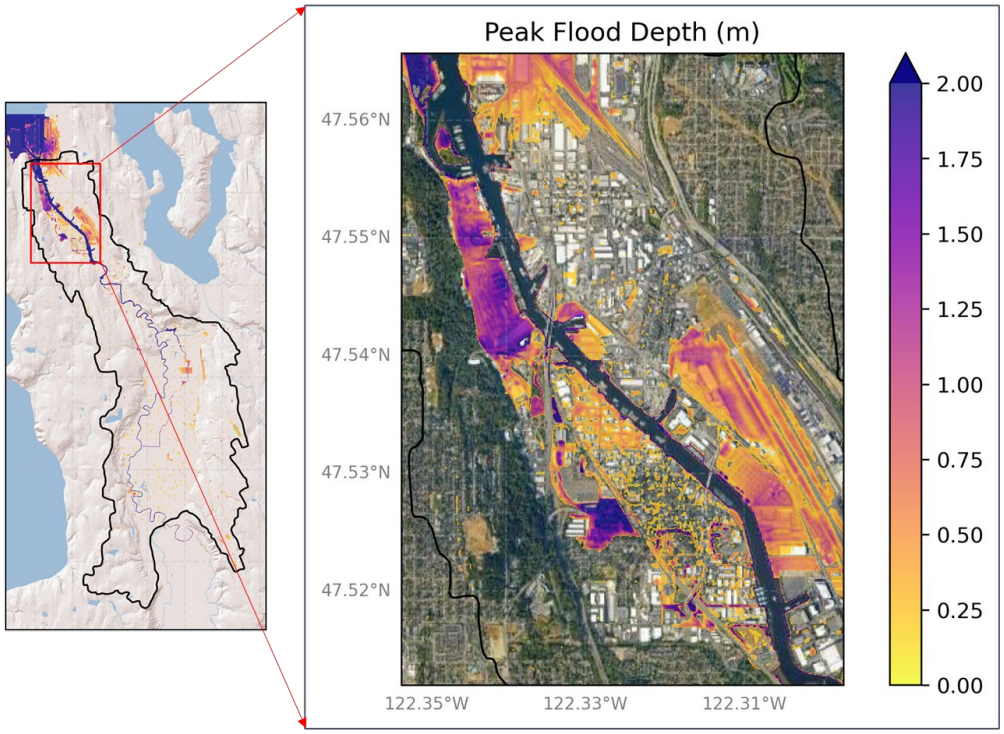

Figure 6. RIFT-simulated peak flood depths (at 10-m resolution) in the most impacted areas of the Lower Duwamish River during the 2022 compound flooding event.

3.2 Multi-Decadal Flood Modeling in the Delaware River and Bay, and Philadelphia

Regional-to-Urban Flood Modeling Performance

The DHSVM-FVCOM-RIFT framework was employed to run long-term simulations (1985-2019) of sub-kilometer integrated fluvial, pluvial, and coastal processes across river, urban, and coastal systems. The model simulations in each of these systems were evaluated against observations, consistently demonstrating good accuracy. Daily series of river discharge simulated by DHSVM were compared with observations from six USGS gauges along the mainstem of the Delaware River (Figure 7). The simulations closely matched the observed flow patterns, with the KGE for daily streamflow ranging from 0.6–0.73.

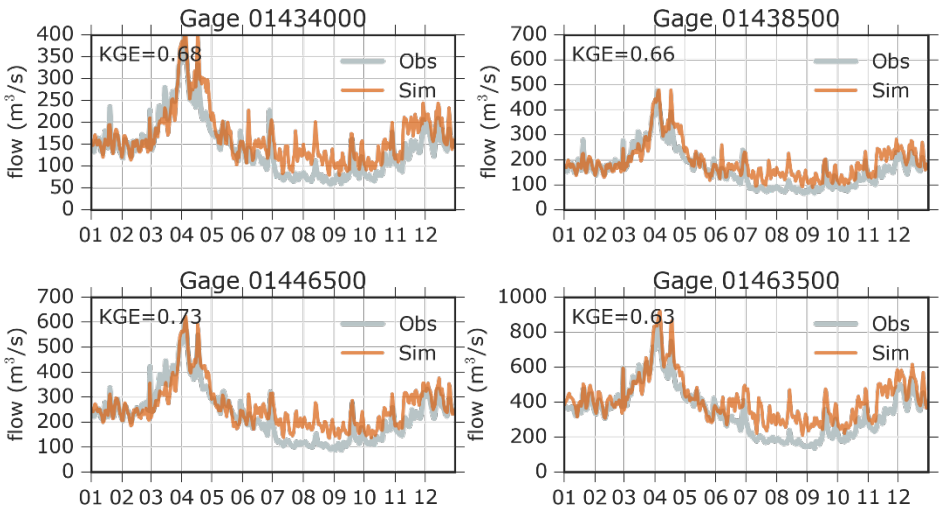

Figure 7. Evaluation of modeled and observed daily streamflow at selected USGS gauges along the Delaware River mainstem. To enhance readability, instead of showing time series, the figure presents mean daily discharges, which are calculated by averaging the daily flows for each calendar day across all simulated years.

WSE simulations from FVCOM were evaluated using hourly WSE observations from various NOAA gauges and generally showed strong agreement (Figure 8). During the five most impactful hurricanes in the region, including Hurricanes Isabel (2003), Wilma (2005), Ernesto (2006), Irene (2011), and Sandy (2012), FVCOM-simulated WSE has correlation coefficients ranging from 0.91–0.97, and mean biases ranging from 0.08–0.18 m.

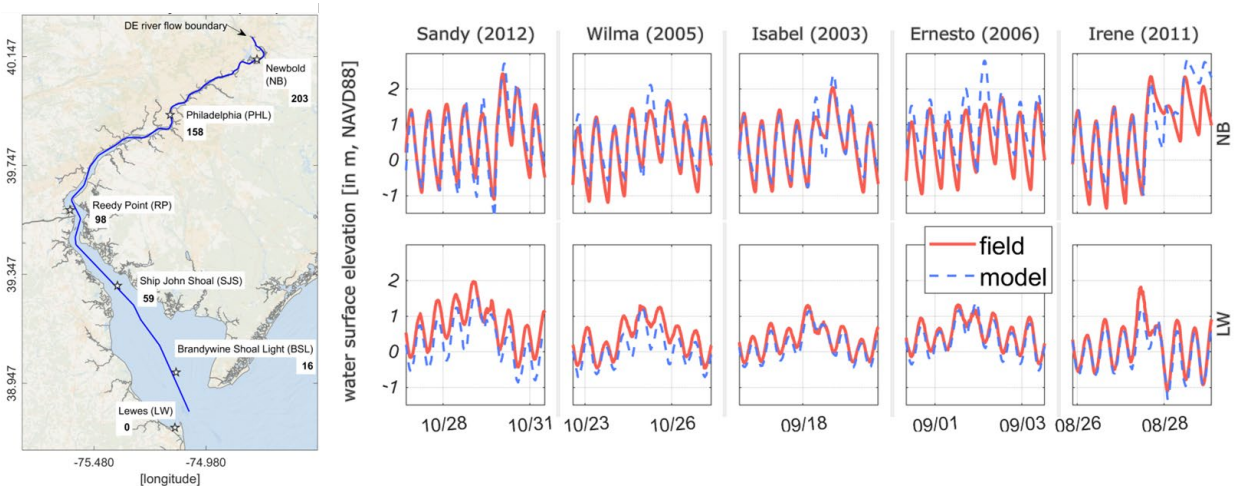

Figure 8. Evaluation of FVCOM-simulated water surface elevation with observations during five major storm events at two NOAA tide gauge locations: Newbold, NJ (NB) in the most upstream Delaware River and Lewes (LW) near the Delaware Bay mouth, as shown on the left map.

We identified a total of 242 flood events impacting Philadelphia based on predefined thresholds for local rainfall, and river and coastal conditions used as RIFT boundary-condition forcings. Due to the absence of high-water mark data, RIFT simulations were evaluated using hourly WSE measurements from two USGS gauges on the Schuylkill River. One gauge is upstream and the other is downstream of

Fairmount Dam. For the periods with available measurements, RIFT was evaluated for 76 flood events post-2007 at the upstream gauge and 28 events post-2016 at the downstream gauge, both showing reasonable accuracy based on several error metrics (Figure 9). For instance, the median correlation coefficients are 0.91 upstream and 0.89 downstream; the median biases in peak flood water depth were -0.02 m upstream and -0.09 m downstream. Notably, RIFT successfully captured the impact of Fairmount Dam, which creates non-tidal conditions upstream and tidal influences downstream, as confirmed by the gauge readings.

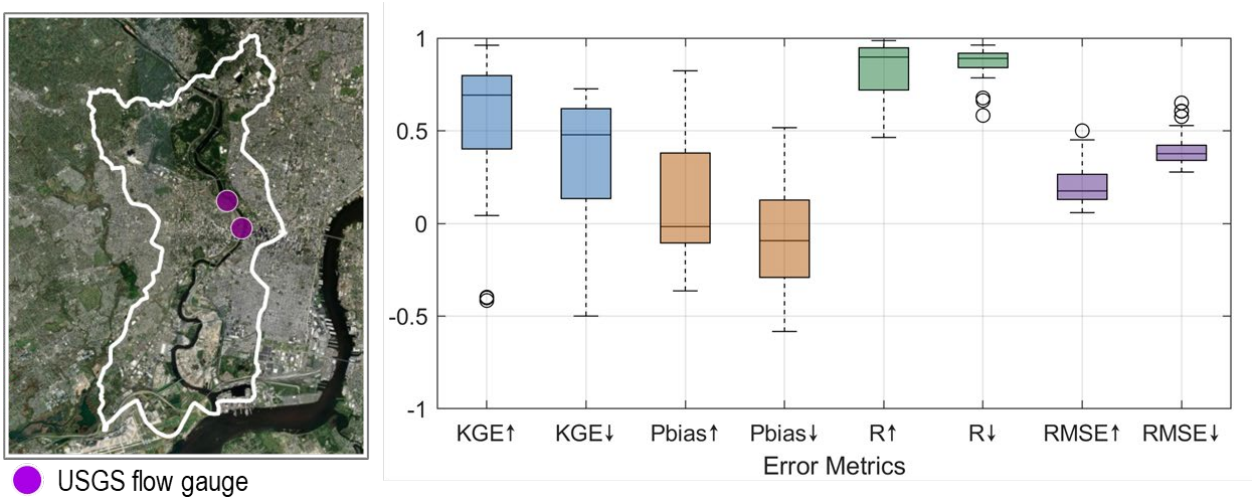

Figure 9. Boxplot showing the evaluation of RIFT simulations for water surface elevation against measurements from two USGS gauges on the Schuylkill River in Philadelphia, as indicated on the left map. The error metrics displayed include Kling-Gupta Efficiency (KGE) and Pearson's correlation coefficient (R), which are dimensionless, and bias in peak water level (Pbias) and root-mean-square error (RMSE), measured in meters. The symbol ↑ on the x-axis indicates metrics for the non-tidal gauge upstream of Fairmount Dam, while ↓ denotes the tidal-influenced gauge downstream.

Prevalence of Compound Flood Drivers in Philadelphia

Among the 242 flood events identified over 35 years, we analyzed the top 70 events with the highest inundated areas. This equates to approximately two events per year, which are considered major flood events. Our analysis identified eight primary drivers of these major flood events, including fluvial-only, pluvial-only, surge-only, and various compound drivers (involving > 1 flood driver).

The circular pie chart (Figure 10) shows the proportional contribution of each flood driver to Philadelphia's major flood events. Notably, 44% of these events result from compound drivers. Furthermore, 30% of these events involve simultaneous flooding from the Schuylkill and Delaware Rivers, combined with surge, rain, or both. Specifically, storm surges frequently coincide with simultaneous river flooding in these two rivers, contributing to 18% of events, primarily during fall and winter. Only 6% of flood events are caused by surge-only, typically affecting near-coast areas without extending inland. Pluvial factors contribute to 27% of events, with pluvial-only (local heavy rainfall) being the cause of 15%, primarily in summer. Combined pluvial and river flooding in both rivers account for 9% of events, frequently in fall. Overall, river flooding plays a significant role in Philadelphia flooding, contributing to 73% of events, either as a single driver or as a component in compound driver cases. Three "All" compound flood events were identified involving concurrent surge, pluvial flooding,

and river flooding in both rivers. These events include Hurricane Irene (August 2011), Hurricane Floyd (September 1999), and the Northeast Winter Storm (April 2007). This analysis highlights the complexity of flood drivers in Philadelphia, emphasizing the need for models that accurately represent the interactions between various flood drivers. Effective flood management in this context requires integrated strategies that consider these multifaceted flood contributing factors.

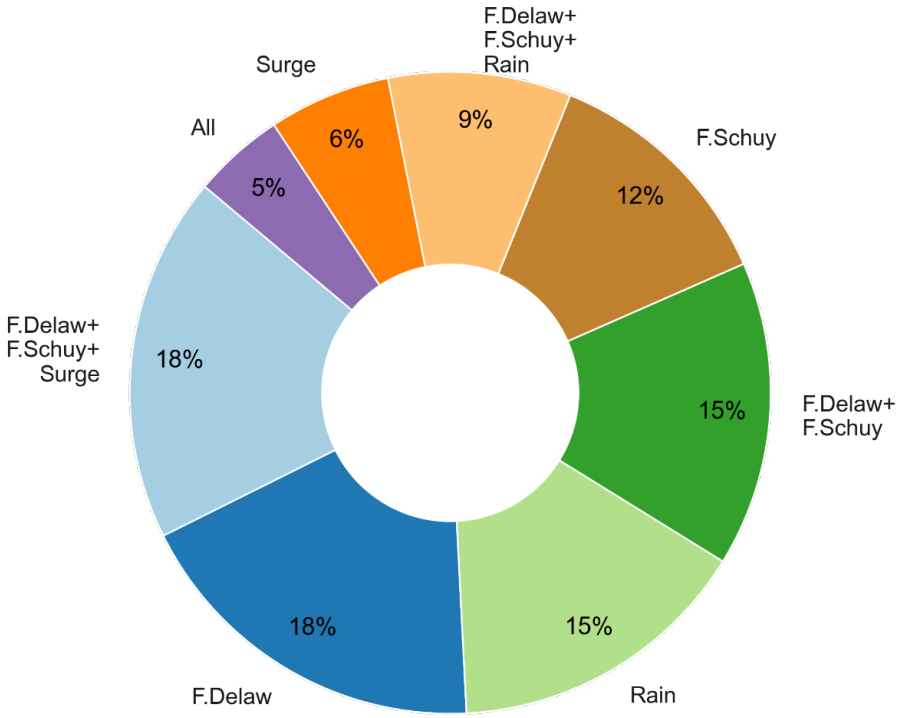

Figure 10. The proportional contribution of eight primary flood drivers to Philadelphia's major flood events. Notably, 44% of these events result from compound drivers (involving > 1 flood driver). The primary drivers include: pluvial (labeled as *Rain*), storm surge (*Surge*), Delaware River flooding (*F.Delaw*), Schuylkill River flooding (*F.Schuy*), and compound drivers combining these elements, including concurrent river flooding (*F.Delaw+F.Schuy*), river flooding with surge (*F.Delaw+F.Schuy+Surge*), river flooding with rain (*F.Delaw+F.Schuy+Rain*), and all factors combined (*ALL*).

Property-Level Mapping of Flood Hazard and Infrastructure Flood Exposure

The 10-meter modeling of urban inundation in Philadelphia enables detailed assessment of property-level flood vulnerability linked to specific flood drivers. For instance, by analyzing average flooding probabilities at the pixel level during major flood events (Figure 11), we observed significant variation in flood risks across different city areas. These variations arise from the differing spatial patterns and extents of impact of individual or combined flood drivers. Higher flood probabilities are notably present in low-lying areas along the Delaware and Schuylkill Rivers, particularly in South and Southwest Philadelphia where Schuylkill River converges with the Delaware River, making these areas susceptible to pluvial, fluvial, and surge impacts. Additionally, pluvial flooding impacts more inland areas not directly adjacent to major rivers, such as neighborhoods in West Philadelphia.

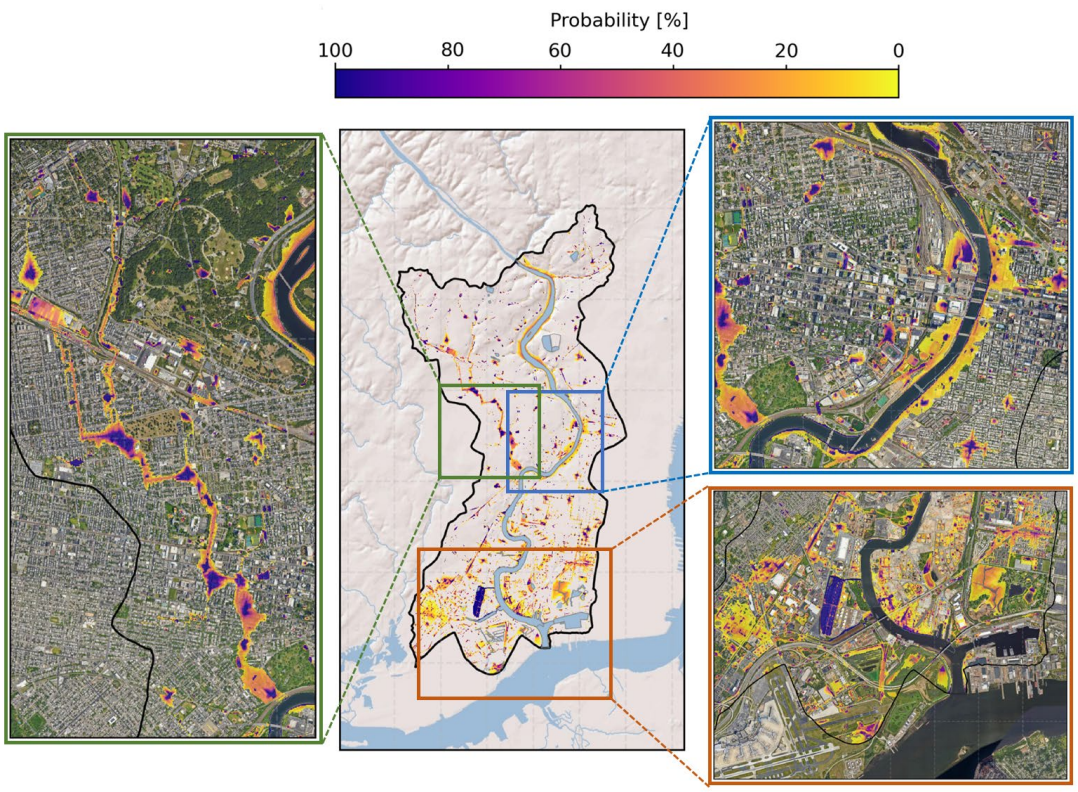

Figure 11. Flood probability mapping of Philadelphia at 10-meter resolution. The central map shows the flood probability across the city, while the inset panels zoom into areas particularly susceptible to flooding.

We further assessed the flood exposure of critical infrastructure, using occupancy type information from the National Structure Inventory (NSI) and infrastructure polygons from the USGS National Structures Dataset. For each infrastructure type (e.g., banks, hospitals, emergency response facilities, and schools), we calculated the average inundated areal fraction over 70 major flood events with a flood depth threshold set to 0.15 m. For more concise results, infrastructure types were grouped by their respective damage category: commercial, industrial, public, or residential. Among these, residential infrastructure was most affected, with an average inundated areal fraction of 0.2, indicating that 20% of these facilities' areas were inundated during major flood events. Notably, industrial infrastructure, a critical asset category, is predominantly located in high-probability flood zones along the Schuylkill River in South Philadelphia (Figure 12), with an average inundated areal fraction of ~10%. Analysis of the contributions of each flood driver to flood exposure for each damage category indicates that industrial, commercial, and residential areas are primarily impacted by pluvial flooding, while public areas are most affected by compound riverine and coastal flood drivers (*F.Delaw+F.Schuy+Surge*).

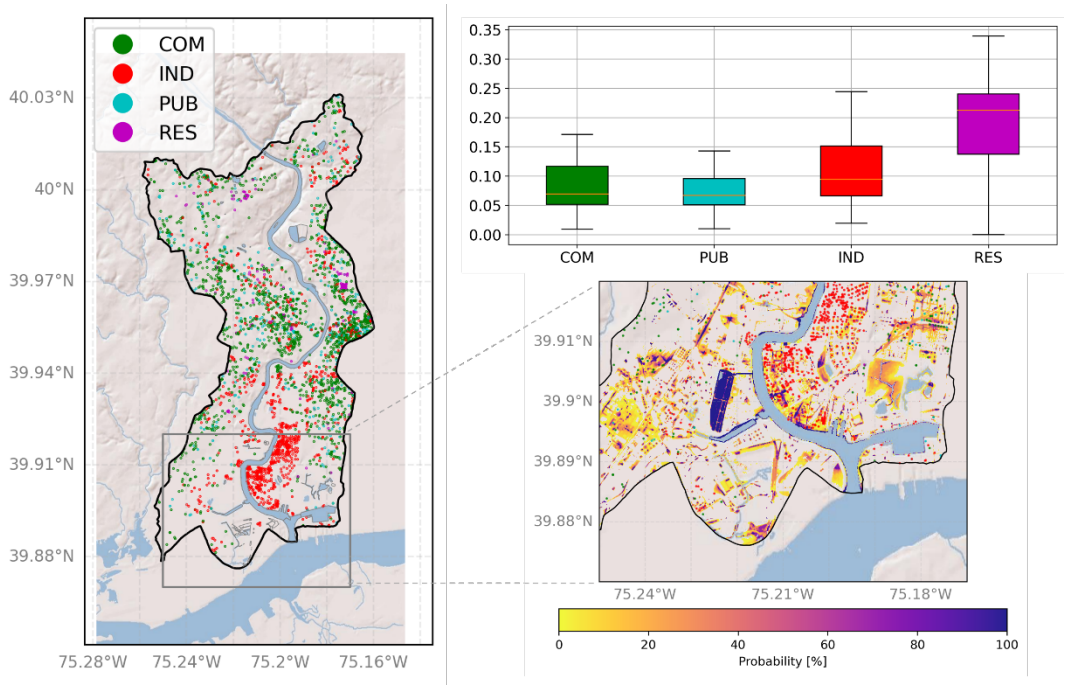

Figure 12. (a) Point locations of critical infrastructure grouped by damage categories: commercial (COM), industrial (IND), public (PUB), and residential (RES); (b) boxplot showing the inundated areal fraction for each damage category during major flood events; (c) flood probability of South Philadelphia where industrial properties are densely located.

4.0 Summary

This report clearly demonstrates and evaluates DOE's advancements in regional-to-urban integrated fluvial, pluvial, and coastal flood modeling capabilities. Driven by atmospheric forcing from kilometer- and near-kilometer scale simulations from the DOE SCREAM model and a regional climate model, respectively, this modeling framework consistently demonstrates skillful flood prediction across two distinct U.S. coastal regions—the Delaware region in the Mid-Atlantic and the Puget Sound region in the Pacific Northwest. The physics-based modeling approach enhances our understanding of flood drivers and characteristics, underscoring the importance of capturing the intricate interactions among pluvial, fluvial, tidal, and surge processes. Looking forward, these tools will support projections of future flood hazards and enhance our understanding of potential shifts in flood drivers, which is essential for informing adaptive decisions for flood management and mitigation planning.

5.0 References

1. Changnon, SA. 2008. "Assessment of Flood Losses in the United States." *Journal of Contemporary Water Research & Educ*ation 138(1): 38–44, https://doi.org/10.1111/j.1936-704X.2008.00007.x

2. Davenport, FV, M Burke, and NS Diffenbaugh. 2021. "Contribution of historical precipitation change to US flood damages." *Proceedings of the National Academy of Sciences of the United States of America* 118(4): e2017524118, https://doi.org/10.1073/pnas.2017524118

3. Pielke, RA, and MW Downton. 2000. "Precipitation and Damaging Floods: Trends in the United States, 1932–97." *Journal of Climate* 13(20): 3625–3637, https://doi.org/10.1175/1520-0442(2000)013<3625:PADFTI>2.0.CO;2

4. Gori, A, N Lin, and J Smith. 2020. "Assessing Compound Flooding from Landfalling Tropical Cyclones on the North Carolina Coast." *Water Resources Research* 56(4): e2019WR026788, https://doi.org/10.1029/2019WR026788

5. Zscheischler, J, S Westra, BJJM van den Hurk, SI Seneviratne, PJ Ward, A Pitman, A AghaKouchak, DN Bresch, M Leonard, T Wahl, and X Zhang. 2018. "Future climate risk from compound events." *Nature Climate Change* 8: 469–477, https://doi.org/10.1038/s41558-018-0156-3

6. Raymond, C, RM Horton, J Zscheischler, O Martius, A AghaKouchak, J Balch, SG Bowen, SJ Camargo, J Hess, K Kornhuber, M Oppenheimer, AC Ruane, T Wahl, and K White. 2020. "Understanding and managing connected extreme events." *Nature Climate Change* 10: 611–621, https://doi.org/10.1038/s41558-020-0790-4

7. Xiao, Z, Z Yang, T Wang, N Sun, M Wigmosta, and D Judi. 2021. "Characterizing the Non-linear Interactions Between Tide, Storm Surge, and River Flow in the Delaware Bay Estuary, United States." *Frontiers in Marine Science* 8, https://doi.org/10.3389/fmars.2021.715557

8. Deb, M, N Sun, Z Yang, T Wang, D Judi, Z Xiao, and MS Wigmosta. 2023. "Interacting Effects of Watershed and Coastal Processes on the Evolution of Compound Flooding during Hurricane Irene." *Earth's Future* 11(3): e2022EF002947, https://doi.org/10.1029/2022EF002947

9. Bevacqua, E, D Maraun, MI Vousdoukas, E Voukouvalas, M Vrac, L Mentaschi, and M Widmann. 2019. "Higher probability of compound flooding from precipitation and storm surge in Europe under anthropogenic climate change." *Science Advances* 5(9), https://doi.org/10.1126/aciadv.aaw5531

10. Hallegatte, S, C Green, RJ Nicholls, and J Corfee-Morlot. 2013. "Future flood losses in major coastal cities." *Nature Climate Change* 3: 802–806, https://doi.org/10.1038/nclimate1979

11. Hanson, S, R Nicholls, N Ranger, S Hallegatte, J Corfee-Morlot, C Herweijer, and J Chateau. 2011. "A global ranking of port cities with high exposure to climate extremes." *Climate Change* 104: 89–111, https://doi.org/10.1007/s10584-010-9977-4

12. Hinkel, J, D Lincke, AT Vafeidis, M Perrette, RJ Nicholls, RSJ Tol, B Marzeion, X Fettweis, C Ionescu, and A Levermann. 2014. "Coastal flood damage and adaptation costs under 21st century sea-level rise." *Proceedings of the National Academy of Sciences of the United States of America* 111(9): 3292–3297, https://doi.org/10.1073/pnas.1222469111

13. Hirabayashi, Y, R Mahendran, S Koirala, L Konoshima, D Yamazaki, S Watanabe, H Kim, and S Kanae. 2013. "Global flood risk under climate change." *Nature Climate Change* 3: 816–821, https://doi.org/10.1038/nclimate1911

14. Wigmosta, MS, LW Vail, and DP Lettenmaier. 1994. "A distributed hydrology-vegetation model for complex terrain." *Water Resources Research* 30(6): 1665–1679, https://doi.org/10.1029/94WR00436

15. Chen, T, Q Zhang, Y Wu, C Ji, J Yang, and G Liu. 2018. "Development of a wave-current model through coupling of FVCOM and SWAN." *Ocean Engineering* 164, 443–454, https://doi.org/10.1016/j.oceaneng.2018.06.062

16. Judi, D, S Burian, and T McPherson. 2011. "Two-Dimensional Fast-Response Flood Modeling: Desktop Parallel Computing and Domain Tracking." *Journal of Computing in Civil Engineering* 25(3): 184–191, https://doi.org/10.1061/(ASCE)CP.1943-5487.0000064

17. Jones, AD, D Rastogi, P Vahmani, AM Stansfield, KA Reed, T Thurber, PA Ullrich, and JS Rice. 2023. "Continental United States climate projections based on thermodynamic modification of historical weather." *Scientific Data* 10: 664, https://doi.org/10.1038/s41597-023-02485-5

18. Sun, N, MS Wigmosta, H Yan, H Eldardiry, Z Yang, M Deb, T Wang, and D Judi. 2024. "Amplified Extreme Floods and Shifting Flood Mechanisms in the Delaware River Basin in Future Climates." *Earth's Future* 12(3): e2023EF003868, https://doi.org/10.1029/2023EF003868

19. Yang, Z, and T Khangaonkar. 2010. "Multi-scale modeling of Puget Sound using an unstructured-grid coastal ocean model: from tide flats to estuaries and coastal waters." *Ocean Dynamics* 60: 1621–1637, https://doi.org/10.1007/s10236-010-0348-5

20. Daly, C, M Halbleib, JI Smith, WP Gibson, MK Doggett, GH Taylor, J Curtis, and PP Pasteris. 2008. "Physiographically sensitive mapping of climatological temperature and precipitation across the conterminous United States." *International Journal of Climatology* 28(15): 2031–2064, https://doi.org/10.1002/joc.1688

21. Knapp, KR, MC Kruk, DH Levinson, HJ Diamond, and CJ Neumann. 2010. "The International Best Track Archive for Climate Stewardship (IBTrACS)." *Bulletin of the American Meteorological Society* 91(3): 363–376, https://doi.org/10.1175/2009BAMS2755.1

22. Sun, N, MS Wigmosta, D Judi, Z Yang, Z Xiao, and T Wang. 2021. "Climatological analysis of tropical cyclone impacts on hydrological extremes in the Mid-Atlantic region of the United States." *Environmental Research Letters* 16: 124009, https://doi.org/10.1088/1748-9326/ac2d6a

23. Leung, LR, and Y Qian. 2009. "Atmospheric rivers induced heavy precipitation and flooding in the western U.S. simulated by the WRF regional climate model." *Geophysical Research Letters* 36(3): L03820, https://doi.org/10.1029/2008GL036445

24. Chen, X, LR Leung, M Wigmosta, and M Richmond. 2019. "Impact of Atmospheric Rivers on Surface Hydrological Processes in Western U.S. Watersheds." *Journal of Geophysical Research – Atmospheres* 124(16): 8896–8916, https://doi.org/10.1029/2019JD030468

U.S. DEPARTMENT OF
ENERGY

Office of Science